BIOCHEMISTRY
including biophysical chemistry & molecular biology

Article

pubs.acs.org/biochemistry

Folded Monomers and Hexamers of the Ectodomain of the HIV gp41 Membrane Fusion Protein: Potential Roles in Fusion and Synergy Between the Fusion Peptide, Hairpin, and Membrane-Proximal External Region

Koyeli Banerjee and David P. Weliky*

Department of Chemistry, Michigan State University, East Lansing, Michigan 48824, United States

Supporting Information

ABSTRACT: HIV is an enveloped virus and fusion between the HIV and host cell membranes is catalyzed by the ectodomain of the HIV gp41 membrane protein. Both the *N*-terminal fusion peptide (FP) and *C*-terminal membrane-proximal external region (MPER) are critical for fusion and are postulated to bind to the host cell and HIV membranes, respectively. Prior to fusion, the gp41 on the virion is a trimer in noncovalent complex with larger gp120 subunits. The gp120 bind host cell receptors and move away or dissociate from gp41 which subsequently catalyzes fusion. In the present work, large gp41 ectodomain constructs were produced and biophysically and structurally characterized. One significant finding is observation of synergy between the FP, hairpin, and MPER in vesicle fusion. The ectodomain-induced fusion can be very efficient with only ∼15 gp41 per vesicle, which is comparable to the number of gp41 on a virion. Conditions are found with predominant monomer or hexamer but not trimer and these may be oligomeric states during fusion. Monomer gp41 ectodomain is hyperthermostable and has helical hairpin structure. A new HIV fusion model is presented where (1) hemifusion is catalyzed by folding of gp41 ectodomain monomers into hairpins and (2) subsequent fusion steps are catalyzed by assembly into a hexamer with FPs in an antiparallel β sheet. There is also significant interest in the gp41 MPER because it is the epitope of several broadly neutralizing antibodies. Two of these antibodies bind our gp41 ectodomain constructs and support investigation of the gp41 ectodomain as an immunogen in HIV vaccine development.

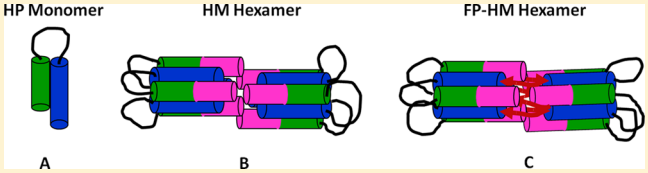

Human immunodeficiency virus (HIV) is enveloped by a membrane obtained during viral budding from an infected host cell. An early step in infection of another cell is fusion of the viral and cell membranes with accompanying release of the viral nucleocapsid into the cytoplasm.[1] The HIV membrane includes a gp160 glycoprotein complex comprised of two noncovalently associated subunits, gp120 and gp41.[2] Gp41 is a ∼350-residue monotopic integral membrane protein with a ∼180-residue ectodomain (Figure 1). Gp120 is bound to the gp41 ectodomain. HIV targets lymphocytes via binding of gp120 to cell receptors and gp120 moves away from or dissociates from gp41. Gp41 then undergoes large conformational changes with accompanying catalysis of membrane fusion. Direct fusion with the plasma membrane has been observed as well as fusion with endosomes following virion endocytosis.[1,3] Fusion appears to occur near physiologic pH via either route. To our knowledge, the gp120/cell receptor complex is only for target cell identification and gp41 is the only fusion protein. Much of our biophysical understanding of fusion has therefore come from studies of gp41 with an emphasis on its ectodomain which can contact the outer leaflets of both the viral and cell membranes. Mutagenesis has demonstrated that there are two ∼20-residue regions of the gp41 ectodomain that play key roles in fusion likely through membrane interaction.[4−6] The N-terminal fusion peptide (FP) and C-terminal membrane-proximal external region (MPER) are postulated to bind to the host cell and viral membranes, respectively. The fusion significances of the FP and MPER have been supported by observation of vesicle fusion induced by FP or MPER peptides. There is an intervening *N*-heptad repeat (NHR), loop, and *C*-heptad repeat (CHR) between the FP and MPER domains (Figure 1).

Electron micrographs of virions show clusters of three gp160, that is, three gp120 and three gp41 molecules. These clusters are likely the initial protein state before any changes in membrane topology because of membrane fusion.[7] The extraviral region of gp160 is termed gp140 and is comprised of gp120 and the gp41 ectodomain without the gp41 TM and gp41 endodomain. WT gp140 is typically monomeric but gp140 trimers can be stabilized via mutations and a gp120/gp41 ectodomain cross-link.[8,9] There are ∼5 Å resolution structures of such gp140 trimers that likely represent the protein state prior to membrane fusion.[10−12] The structure includes a loose bundle of three parallel NHR helices and three CHR helices forming a tripod. The monomer structure is NHR-helix/70°-turn/CHR-helix. The FP and MPER are not in

Received: September 12, 2014
Revised: November 4, 2014
Published: November 5, 2014

   dx.doi.org/10.1021/bi501159w | *Biochemistry* 2014, 53, 7184−7198

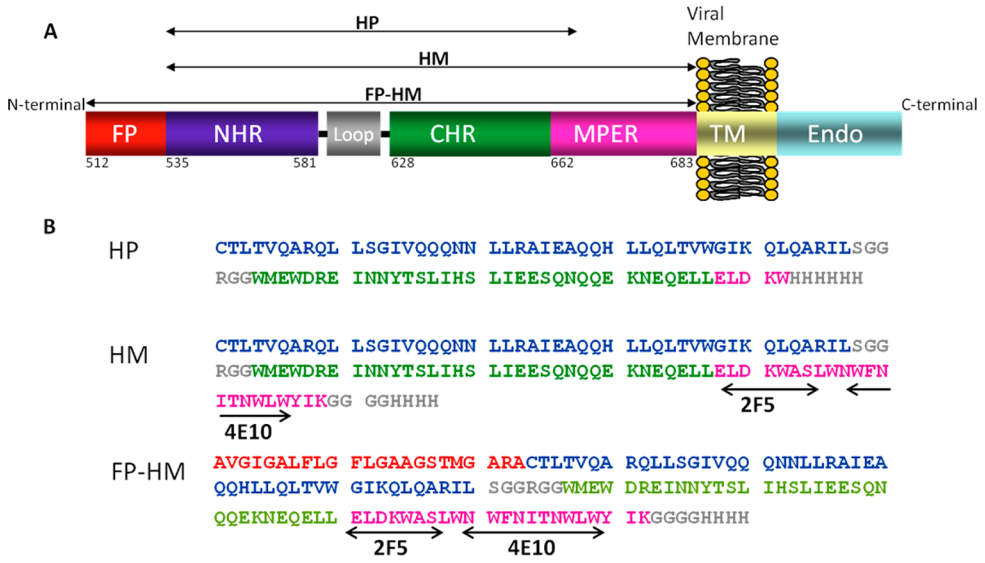

Figure 1. (A) Schematic diagram of HIV gp41 where FP = fusion peptide, NHR = N-heptad repeat; CHR = C-heptad repeat, MPER = membrane-proximal external region, TM = transmembrane domain, and endo = endodomain. (B) Amino acid sequences of HP, HM, and FP-HM. The epitopes of the 2F5 and 4E10 bNAbs are marked.

the structure. There are also atomic-resolution structures of segments of the gp41 ectodomain typically without the FP and MPER and without gp120.[13−16] These show NHR-helix/180°-turn/CHR-helix hairpin structure as well as assembly of three molecules into a six-helix bundle (SHB) with the three NHRs forming parallel coiled-coil structure on the bundle interior and the three CHRs packing antiparallel to the NHRs on the bundle exterior. Melting temperatures of ∼70 °C are observed for shorter ectodomain constructs with hairpin structure whereas temperatures up to 110 °C are observed for longer constructs.[17,18] This thermostability has supported the SHB as the final gp41 structure during fusion.

In addition to the initial NHR/70°-turn/CHR bent structure and the final NHR/180°-turn/CHR SHB structure, a "pre-hairpin intermediate" (PHI) structure has been proposed to form after removal of the gp120s. Each PHI gp41 has a fully extended (no turn) structure, that is, NHR-helix/0°-turn/CHR-helix and there are separate NHR and CHR trimer helical bundles. To our knowledge, the existence of the gp41 PHI is only supported by functional studies, in particular inhibition of membrane fusion and HIV infection with NHR or CHR +MPER peptides.[19,20] These peptides are proposed to bind to the CHR and NHR bundles of the PHI, respectively, and to inhibit the PHI → SHB structural transition. CHR+MPER peptides are a clinically prescribed HIV treatment.[21]

There are also distinct membrane structures during fusion.[22] The separate viral and host cell membranes first merge into a hemifusion intermediate characterized by intermembrane lipid mixing and no contents mixing. This is followed by breaking the hemifusion barrier and formation of a small pore through which small species (e.g., atomic ions) can pass. The fusion pore then expands to create a single membrane enclosing the cell and the viral capsid.

There are little data about the relative timing of gp41 and membrane structural changes. One common **model I** has been: (1) gp120 receptor binding followed by gp120 removal; (2) formation of extended PHI gp41 trimer followed by FP insertion into the host cell membrane; (3) PHI → SHB trimer folding that brings the two membranes close together; (4) hemifusion; (5) initial pore formation; and (6) fusion pore expansion.[23] The appealing intuitive aspect of this model is that some of the free energy released during PHI → SHB folding is used to form membrane intermediates. However, the relative timings of this model are not supported by the observation that CHR+MPER peptides inhibit fusion up to the final fusion pore expansion step.[20] Because the peptides are presumed to bind to the PHI trimer but not the SHB trimer, these data suggest an alternative **model II**: (1) gp120 receptor binding followed by gp120 removal; (2) formation of extended PHI gp41 trimer followed by FP insertion into the host cell membrane; (3) hemifusion; (4) initial pore formation; (5) PHI → SHB trimer folding; and (6) fusion pore expansion.[24]

In the present work, we show that the gp41 ectodomain can form stable hairpin monomers as well as stable hexamers that are likely composed of two SHB trimers. CHR+MPER inhibitor peptides likely bind to the monomer but not the trimer or hexamer. These findings are the basis of a new **model III** (Figure 12): (1) gp120 receptor binding followed by gp120 removal; (2) dissociation of gp41 ectodomain into monomers and formation of extended PHI gp41 ectodomain monomer followed by FP insertion into the host cell membrane; (3) PHI → hairpin monomer folding that brings the two membranes close together; (4) hemifusion; (5) initial pore formation; (6) hairpin monomer → SHB trimer → hexamer ectodomain assembly; and (7) fusion pore expansion. Like **model I** and unlike **model II**, the new **model III** retains the appealing coupling of the PHI → SHB transition to initial steps of membrane fusion. There are more reasonable coordinated changes of the ectodomain and membrane topologies for PHI → SHB monomer folding of **model III** than for PHI → SHB trimer folding of **models I** and **II**. Finally, the discovery of stable hexamers correlates with other data supporting a requirement of multiple gp160 trimers for membrane fusion and HIV infection.[25,26]

Much of our understanding of the FP and MPER regions of the gp41 ectodomain has been based on studies of vesicle fusion induced by peptides.[27−29] Rapid (∼5 s) fusion typically requires 500−1000 peptides per ∼100 nm diameter vesicle

dx.doi.org/10.1021/bi501159w | *Biochemistry* 2014, 53, 7184−7198

which is much higher than the ∼30 gp160 per virion and suggests that there are aspects of viral fusion unaccounted for in the peptide studies.[30] A reasonable hypothesis with some supporting data is that the rest of the ectodomain plays an important role in fusion. In the present work, we demonstrate efficient vesicle fusion with only ∼15 gp41 per vesicle provided that the FP, hairpin, and MPER are included in the large gp41 ectodomain construct. To our knowledge, this is the first demonstration of fusion synergy between the FP, hairpin, MPER in a large gp41 ectodomain construct. Such synergy correlates with postulated binding of FP and MPER regions to host cell and viral membranes, respectively, and also with postulated FP/MPER interaction in a folded hairpin structure.

The MPER is the epitope of several broadly neutralizing antibodies (bNAbs) that prevent infection by diverse isolates of HIV.[5,31] There has consequently been continued effort to develop a HIV vaccine with a MPER immunogen. The ectodomain with MPER and hairpin structure is a candidate immunogen in part because of the stability of this structure. However, there is disagreement in the literature about the antigenicity of the hairpin, that is, whether bNAbs bind well to the MPER in this structure.[32−34] The present study shows such binding for the hairpin ectodomain which is initially in a monomer or hexamer state.

MATERIALS AND METHODS

HP and HM Inserts. Amino acid (Figure 1B) sequences are for the HXB2 laboratory strain of HIV and are described using gp160 numbering (see Supporting Information for DNA sequence). HP and HM include the NHR residues 535-(M535C)-581 and a non-native loop (SGGRGG). HP includes CHR residues 628−666 and a non-native H_6 tag. HM includes CHR+MPER residues 628−683, a non-native G_4 spacer, and a non-native H_4 tag. The HP insert in the pGEM-t vector without the H_6 tag has been previously described and the H_6 tag was then added via PCR.[35] The HM insert was generated from the HP insert via multiple rounds of PCR.

HP and HM Expression, Solubilization, and Purification. The expression host was *Escherichia coli*, BL21(DE3) strain. The typical protocol began with addition of 1 mL of bacterial glycerol stock to 50 mL of LB medium. After overnight growth at 37 °C, the 50 mL culture was added to 1 L of fresh LB medium. Growth was continued for 2 h with a final OD_{600} of ∼0.8. Protein expression was induced with addition of 2 mM IPTG and continued for 6 h at 37 °C. "Pellet I" (∼9 g) was harvested by centrifugation at 9000*g*. The next steps were done at 4 °C using 30 mL PBS at pH 7.4 with protease inhibitor cocktail. Three g of pellet I was suspended in PBS and lysed by tip sonication in an ice bath. The lysate was centrifuged at 48000*g* and the resultant "pellet II" was sonicated in PBS with subsequent centrifugation. SDS-PAGE showed that the resultant "pellet III" had a high mass fraction of recombinant protein (RP). Pellet III was effectively solubilized by sonication in PBS + 6 M GuHCl and the RP in this solution was purified at ambient temperature by affinity chromatography with Co^{2+} resin. The resin suspension solutions were PBS (pH 7.4) + 6 M GuHCl + imidazole and resin was isolated using gravity filtration. After initial protein binding with 1 mM imidazole, weakly bound proteins were removed using sequential washes with 5 mM imidazole (2×), 10 mM imidazole (2×), and 20 mM imidazole (2×). The RP was eluted using 250 mM imidazole (4 ×) and the purified yields of HP and HM were ∼50 and ∼15 mg/L culture, respectively, as determined by A_{280}. Elutions were (1) diluted to ∼0.1 mg RP/mL in PBS + 6 M GuHCl + 2 mM DTT; (2) dialyzed at 4 °C against 50 mM sodium formate buffer (pH 3.2) + 150 mM NaCl + 0.2 mM TCEP reducing agent; and (3) concentrated to ∼1 mg/mL. HP and HM were aggregated in the pH 5−9 range in the absence of GuHCl. Aggregation of either protein was evidenced by a visibly significant quantity of protein precipitate.

Synthesis and Purification of FP-HM. FP23 (residues 512−534 (S534A)-(thioester linker)) was synthesized manually by t-boc chemistry, purified by RP-HPLC, and quantitated with the BCA assay. Purity was >95% by MALDI MS. Native chemical ligation between FP23 and HM was done with 1.2 mM FP23, 1.2 mM HM, 0.1 M sodium phosphate buffer at pH 7.2, 8 M GuHCl, 60 mM MPAA, 2 mM TCEP, 1 day time, and ambient temperature. The ligation products were purified by RP-HPLC.

Size-Exclusion Chromatography (SEC). A DuoFlow Pathfinder 20 instrument (Bio-Rad) was used with a flow rate of 0.3 mL/min, A_{280} detection, and Tricorn semi-preparative columns (GE Technologies).

CD Spectroscopy. A Chirascan spectrometer (Applied Photophysics) was used with a quartz cuvette with 1 mm path length. There were 0.5 nm steps with 1.5 s per step. For each sample, three scans were averaged. The final spectrum was the (RP + buffer) − buffer difference spectrum.

Western Blots. Purified RP in SDS buffer (∼0.5 mg/mL) was boiled followed by SDS-PAGE (∼5 μg RP per lane) and transfer to a nitrocellulose membrane and incubation in a 10 mL solution containing antibody (5 μg), TBST at pH 7.4, and 5% w/v nonfat dry milk. Subsequent incubation with Goat Anti-Hamster IgG (H+L) HRP conjugate secondary antibody (1 μg) was followed by development with SuperSignal West Pico chemiluminescent substrate.

Immunoprecipitation. Five microgram quantities of RP and antibodies were used from 1 mg/mL stocks. Solutions other than RP stock contained PBS at pH 7.4. bNAb was incubated with Protein G magnetic beads followed by 3× wash removal of free bNAb. Because RP binds to unpassivated beads but not IgG, the beads were incubated with IgG and then washed. The beads were then incubated with RP in 700 μL solution for 1 h and washed. Bound RP and antibodies were removed by boiling in SDS sample buffer and analyzed by SDS-PAGE.

Protein-Induced Vesicle Fusion. Lipid:Chol (1.0:0.5 μmole) was dissolved in chloroform followed by chloroform removal with nitrogen gas and vacuum pumping. The film was homogenized by freeze−thaw cycles in ∼1 mL buffer and extruded through 100 nm diameter pores to form unilamellar vesicles. Fluorescently labeled vesicles were similarly prepared except that the mixture also contained 2 mol % of the fluorescent lipid *N*-NBD-PE and 2 mol % of the quenching lipid *N*-Rh-PE. Labeled and unlabeled vesicles were mixed in 1:9 ratio with total [lipid+Chol] ≈ 230 μM. Fluorescence of the stirring vesicle solution was measured at 37 °C with 467 nm excitation, 530 nm detection, and 1 s time increment. After measurement of the baseline fluorescence F_0, a protein aliquot was added and marked time $t = 0$. Vesicle fusion was reflected in the increased fluorescence $\Delta F(t) = F(t) - F_0$ because of longer distances between fluorescent and quenching lipids in a fused (labeled+unlabeled) vesicle relative to the initial labeled vesicle. The dead-time in the assay was ∼5 s and asymptotic fluorescence (ΔF_f) was usually reached by ∼600 s. The maximum fluorescence change (ΔF_{max}) was detected after

dx.doi.org/10.1021/bi501159w | *Biochemistry* 2014, 53, 7184−7198

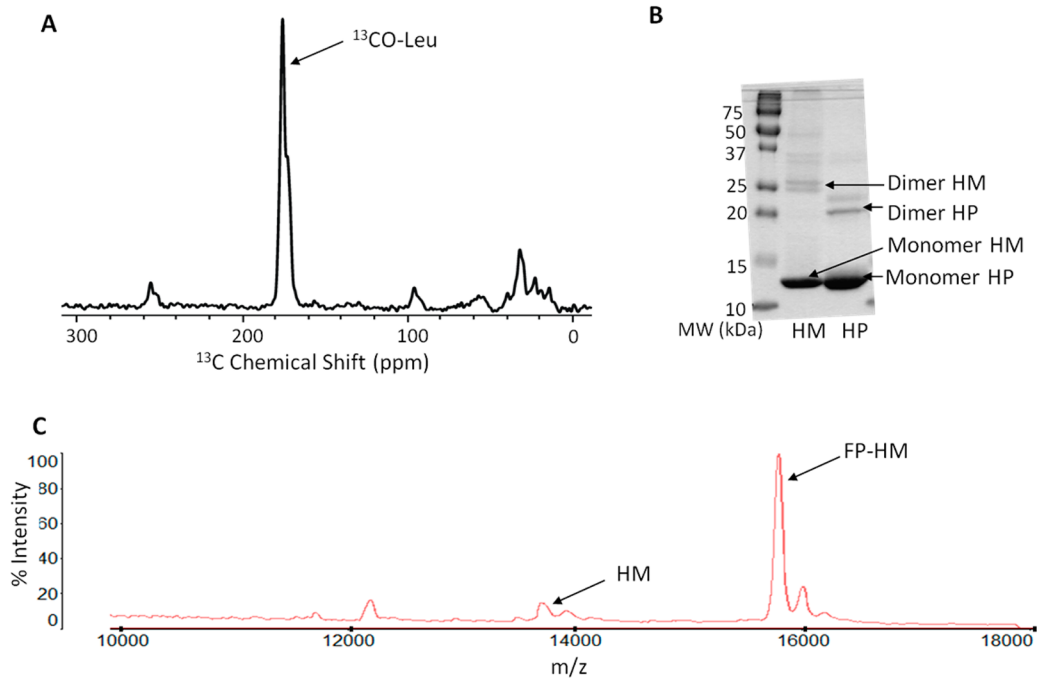

Figure 2. (A) ^{13}C SSNMR spectra of a cell pellet harvested from centrifugation of a cell lysis in PBS. The *E. coli* cells contained a plasmid with the HM insert and expression was induced for 2 h in minimal medium containing ^{13}CO-Leu. Any expressed HM will therefore be ^{13}CO-Leu labeled. The SSNMR acquisition parameters included a 9.4 T magnetic field, 4 mm diameter rotor, 8 kHz magic angle spinning frequency, and ∼1 day of signal averaging. The ratio of integrated isotropic ^{13}CO intensity (peaked at ∼175 ppm) to integrated aliphatic intensity (0−90 ppm region) translates to expression of ∼300 mg HM/L culture. (B) SDS-PAGE of purified HM (MW = 13.7 kDa) and HP (MW = 11.6 kDa). (C) MALDI MS of FP-HM ligation product twice-purified by RP-HPLC. The experimental ratio $[m/z(\text{FP-HM})/m/z(\text{HM})]$ is 1.1522 and matches the ratio of expected MWs, [MW(FP-HM)/MW(HM)] = 1.1522.

addition of 12 μL 10% Triton X-100 which solubilized the vesicles. Percent fusion was $M(t) = \{\Delta F(t)/\Delta F_{max}\} \times 100$. Comparison among assay replicates showed $\delta(M_f)/M_f \approx 0.02$.

We wanted to compare vesicle fusion induced by HP, HM, and FP-HM where all proteins were in the same stock buffer conditions. FP-HM was not soluble without 6 M GuHCl, so the chosen stock conditions were 10 mM sodium formate at pH 3.2, 6 M GuHCl, and 0.2 mM TCEP. The effects of the stock pH and GuHCl were minimized by always adding 7.5 μL of stock into a final total volume of 1200 μL with final [GuHCl] = 40 mM. Vesicle fusion was done for final pHs of 3.2 and 7.4 with respective stock [protein] = 20 μM and 160 μM, chosen so that (1) for all proteins, M_f < 100% with no light scattering; and (2) for at least one protein, M_f was appreciably greater than 0%.

RESULTS

High-Yield Protein Production. Cells that had expressed HP were lysed in PBS but SDS-PAGE of the soluble lysate did not show a clear HP band. It was therefore concluded that most of the HP was in inclusion bodies (IBs). After an additional lysis in PBS, different solubilization conditions were tested for "pellet III" as defined in the Experimental section. Similar intensity HP bands were observed in SDS-PAGE of the lysates from glacial acetic acid, 1% w/v SDS, 8 M urea, or 6 M GuHCl. Purification of the 6 M GuHCl lysate yielded HP with high purity (Figure 2B). The most intense band was the HP monomer and there were also reproducible weaker dimer bands confirmed to be HP by Western blotting with anti-His tag antibody. The purified yield was ∼50 mg HP/L culture.

The first HM construct had a H_6 C-terminal tag without glycines and the initial efforts to solubilize and purify the protein were unsuccessful as judged by no clear band in SDS-PAGE. It was unclear whether the main problem was low expression, low solubilization, or purification losses. HM expression prior to solubilization was then quantitated with a recently developed solid-state NMR (SSNMR) method.[36] Addition of ^{13}CO-Leu during the expression period resulted in ^{13}CO-labeling of HM. Cells were lysed in PBS followed by centrifugation of the lysate and the harvested pellet was enriched in any HM IBs. The ^{13}C NMR spectrum of this pellet showed a prominent ^{13}CO feature consistent with ∼300 mg HM/L in IBs (Figure 2A). The main bottlenecks to purified HM were therefore low solubilization of HM IBs or purification losses.

A systematic search was carried out to find conditions for solubilization of HM IBs. Two sequential lyses were done in PBS to solubilize other proteins. Assessment of solubilization of HM IBs in pellet III was done by (1) visual reduction in pellet size; and (2) SDS-PAGE of the solution. Many conditions that solubilized HP IBs did not solubilize HM IBs. Appreciable HM solubilization was only achieved with 1% SDS or 6 M GuHCl and the latter additive was chosen for solublization and purification. HM with H_6 tag did not bind the Co^{2+} resin whereas HM with a G_4H_6 tag bound so tightly that there was no elution with 250 mM imidazole. HM with a G_4H_4 tag both bound tightly to the resin with 20 mM imidazole and also eluted from the resin with 250 mM imidazole. The purified yield was ∼15 mg HM/L culture and SDS-PAGE showed dominant monomer and weaker dimer bands (Figure 2B).

FP-HM was produced by native chemical ligation between FP and HM and purified by RP-HPLC. For one round of

dx.doi.org/10.1021/bi501159w | *Biochemistry* 2014, 53, 7184−7198

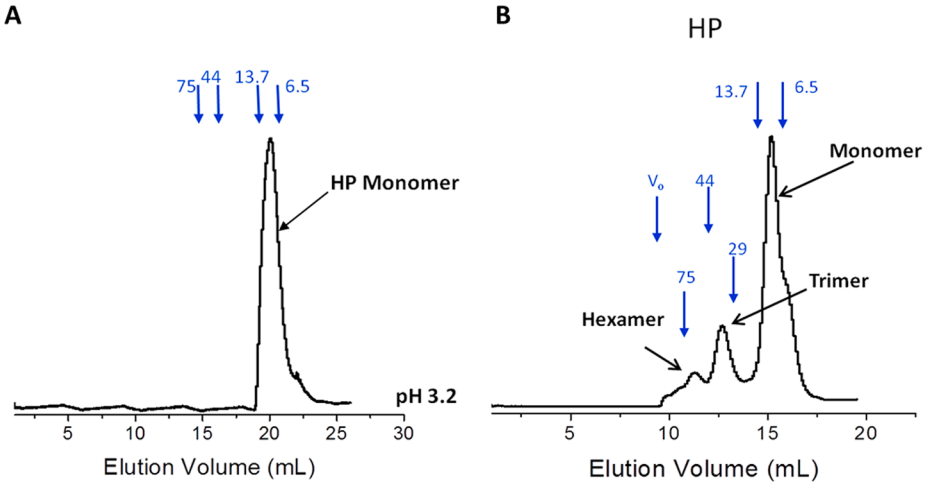

Figure 3. SEC A_{280} profiles for HP with (A) 1 mg/mL loading, Superdex 200 column and (B) 10 mg/mL loading, Superdex 75 column. The loading and running buffer was 50 mM sodium formate pH 3.2, 150 mM NaCl, and 0.2 mM TCEP. The blue numbers are the MW standards in kDa and their respective elution volumes are the downward blue arrows. There are accompanying SEC profiles of the MW standards, as well as plots of K_{av} vs $\log_{10}$(MW) (Supporting Information).

purification, MS intensities showed FP-HM:HM ≈ 1.2 which correlated with SDS-PAGE (Supporting Information). For two rounds of RP-HPLC, the FP-HM:HM ≈ 10 (Figure 2C). However, there was too little FP-HM, so the FP-HM+HM mixture after only one round was used for subsequent experiments.

Solubility Only at pH 3 or with 6 M GuHCl. Solubility in a particular buffer was examined by (1) dialyzing the protein (~0.2 mg/mL) against the buffer for 1 day; (2) centrifugation at 16000*g* for 5 min; and (3) measuring protein concentration in the supernatant. A protein was typically either soluble by the criterion [final concentration]/[initial concentration] > 0.8 or poorly soluble with obvious precipitation.

None of the proteins were soluble in (1) 10 mM sodium formate at pH 5.0; (2) 5 mM HEPES/10 mM MES at pH 7.4; (3) PBS at pH 7.4 with or without 0.1% (w/v) nonionic detergent (Triton X-100, *N*-lauroylsarcosine, *n*-decyl-*β*-D-maltopyranoside, and *n*-dodecylphosphocholine were tested); or (4) 10 mM Tris at pH 9.0. Both HP and HM were soluble in 10 or 50 mM sodium formate buffer at pH 3.2. However, FP-HM was not soluble under these conditions. All proteins were soluble with 6 M GuHCl at either pH 3.2 (50 mM sodium formate) or pH 7.4 (10 mM sodium phosphate). There was solubility either with or without 150 mM NaCl. At pH 7.4, there was no appreciable solubility with [GuHCl] < 6 M.

Monomer or Hexamer and Not Trimer. Oligomerization was probed by SEC for conditions that satisfied the above solubility criteria. The typical protein loading was 1 mg/mL, and there was ~10-fold dilution in the column. For a particular buffer, the dominant oligomeric state was either monomer or hexamer and never trimer. For example, for HP at pH 3.2 without GuHCl, the SEC profile is consistent with a monomer (Figure 3A). This is significant as CD, calorimetric, and vesicle fusion studies of gp41 ectodomain constructs have often been done with protein at pH 3.[18,35,37] It has typically been assumed that there are SHB trimers; however, the SEC only shows monomers. For 10 mg HP/mL loading concentration, the SEC profile also shows a major fraction monomer with much smaller fractions of trimers, hexamers, and larger aggregates (Figure 3B). SEC was attempted for HM at pH 3.2 without GuHCl but the protein bound to the Superdex column material. For buffer with 6 M GuHCl at either pH 3.2 or pH 7.4, both HP and HM show major fraction hexamer with much smaller fractions assigned to dodecamers, 24-mers, and aggregates with MW > 2 MDa (Figure 4). Although cell physiology does not include 6 M GuHCl, it is the only condition we found that resulted in a defined small oligomer state. The hexamer is also the dominant species when non-native protein tags are added to the ectodomain construct.[38] We therefore used 6 M GuHCl as one initial solubilization condition in subsequent experiments. The major hexamer population and minor populations of larger oligomers likely represent a thermodynamic equilibrium state. This was evidenced by collecting the hexamer fraction, concentrating to 1 mg/mL, and then reloading this fraction for a second round of SEC. The resultant SEC profiles for HP and HM are similar to those initially observed (Supporting Information).

Hyperthermostable Hairpin Structure of the Monomer. CD spectra of HP and HM at pH 3.2 without GuHCl have the 208/222 nm minima characteristic of *α* helical structure and the θ_{222} values are consistent with dominant helical structure (Figure 5A). HP is predominantly a monomer in this buffer so the data support a highly helical monomer. There is a small fraction of trimer for high SEC loading and the CD spectrum of this fraction is also consistent with dominant helical structure. The ~15% reduction in $|\theta_{222}|$ of trimer relative to monomer is not understood. For HM, there was a small linear decrease in $|\theta_{222}|$ between 20 and 95 °C (Figure 5B) that is similar to the previously observed temperature-dependence for HP and other large ectodomain constructs at pH 3. This correlates with calorimetrically determined T_m values of ~110 °C.[18]

CD spectra for the D632A and D632A/W628A mutants of HP provide additional support for the helical monomer model (Figure 5C). In the atomic-resolution SHB trimer structure, D632 and W574 form an intermonomer CHR/NHR salt bridge and W628 and W571 form an intramonomer hydrophobic interaction.[39] There is negligible difference between the WT and D632A CD spectra whereas there is about two-times less magnitude molar ellipticity in the D632A/W628A spectrum that is consistent with a significant loss in helicity. These data support hairpin monomer structure of HP which is

dx.doi.org/10.1021/bi501159w | *Biochemistry* 2014, 53, 7184−7198

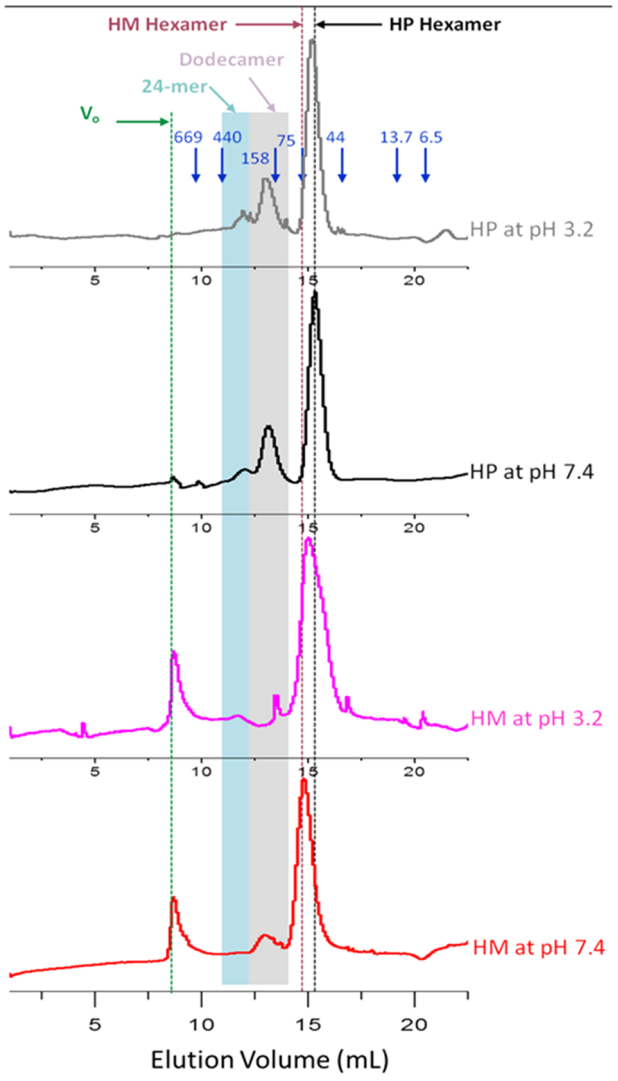

Figure 4. SEC A_{280} profiles from a semipreparative Superdex 200 column for HP and HM in buffers containing 6 M GuHCl and 150 mM NaCl. The pH 3.2 buffer was 50 mM sodium formate with 0.2 mM TCEP and the pH 7.4 buffer was 10 mM phosphate with 2 mM DTT. For each run, the loading and running buffers were the same and the loading stock solution had a 1 mg/mL protein concentration. The blue numbers are the MW standards in kDa and their respective elution volumes are the downward blue arrows. The most prominent peaks in the profiles correspond to hexamer masses and vertical dashed lines show the elution volume offset between the HP and HM hexamers. Smaller peaks most consistent with dodecamer and 24-mer masses are identified by shaded regions. For HM, there is also a small peak associated with the V_o void volume, that is, aggregates with MW $\geq$ 2 MDa.

similar to a monomer unit of the SHB trimer structure (Figure 11A). The T_m of ~110 °C corresponds to unfolding of hairpin monomer rather SHB trimer.

For HP and HM in 6 M GuHCl at either pH 3.2 or pH 7.4, there is a 222 nm minimum consistent with helical structure (Figure 5D). Significant absorption/interference from the GuHCl precludes quantitation of the helical fraction. The hexamer is the dominant oligomeric state under these conditions and may be a dimer of two SHB trimers. For HP in 6 M GuHCl at pH 7 between 20 and 90 °C, there is a linear decrease in $|\theta_{222}|$ comparable to Figure 5B change without GuHCl. This supports thermostability of the hairpin monomer structure within the hexamer.

The ligations are done in 8 M GuHCl at pH 7 and ambient temperature so it is interesting to consider the structural properties in this condition. For HP in 8 M GuHCl at 20 °C, the $|\theta_{222}|$ is about 60% of the value in 6 M GuHCl. In addition, the $|\theta_{222}|$ in 8 M GuHCl exhibits a small linear decrease between 20 and 70 °C. These data are consistent with a dimer of SHB trimers in 8 M GuHCl.

Hairpin Monomer with MPER is Highly Fusogenic. Earlier work has shown that peptides corresponding to the FP and the MPER regions induce vesicle fusion.[27,29] For the present study, we investigated the effects of these regions as part of the gp41 ectodomain including the hairpin region. The typical vesicle composition was POPC:POPG:Chol (8:2:5) and reflected the major fraction PC, minor fraction negatively charged lipid, and mole fraction Chol in the membranes of HIV and its host cells.[40] Fusion was studied at final pHs of 3.2 and 7.4 which was motivated by previous studies with HP showing much greater fusion of negatively charged vesicles at pH 3.2 relative to pH 7.4.[41] A second vesicle composition was POPC:DOTAP:Chol (8:2:5) and contained positively charged DOTAP rather than negatively charged POPG. Comparison of results for the two compositions and two pH values provides insight into the role of protein/vesicle electrostatics because the POPG and DOTAP are respectively negatively and positively charged at both pH values, whereas the protein is positively charged at pH 3.2 and negatively charged at pH 7.4.

HP and HM were solubilized as monomers at pH 3.2 and induced rapid fusion of negatively charged POPG vesicles at this pH with low 1:700 protein:total lipid mole ratio (Figure 6A). This is likely monomer-induced fusion because of insufficient time for oligomerization at the membrane surface prior to fusion. At pH 7.4, comparable fusion required an order-of-magnitude higher 1:75 ratio (Figure 6B). For 1:150 ratio, there was negligible fusion which is consistent with earlier work. For positively charged DOTAP vesicles, there was little fusion at pH 3.2, measurable fusion at pH 7.4, and higher fusion at pH 9.0 (Figure 6C and D). The different pH dependences for POPG and DOTAP vesicles likely reflect differences in protein/vesicle electrostatic energy, that is, (1) attractive energy between the positively charged protein and negatively charged POPG vesicles at low pH and between the negatively charged protein and positively charged DOTAP vesicles at neutral and high pH and (2) repulsive energy between the negatively charged protein and negatively charged POPG vesicles at neutral pH and between the positively charged protein and positively charged DOTAP vesicles at low pH. Attractive energy results in a higher fraction bound protein and repulsive energy results in a lower fraction. In the spatially restricted environment of HIV/host cell fusion, there is likely high protein/membrane binding that is similar to near-quantitative binding during the pH 3.2 vesicle fusion of POPG vesicles. Higher fusion extent for POPG vesicles at low pH relative to DOTAP vesicles at neutral and high pH may be a consequence of the different magnitudes of attractive electrostatic energy. This hypothesis is evidenced by calculated hairpin charges of about +10 at pH 3.2, −2 at pH 7.4, and −4 at pH 9.0. For many data, fusion was rapid and occurred during the ~5 s dead-time of the assay which is consistent with earlier studies. Other studies have also shown that as the fraction of charged lipid in the vesicle is decreased, the fusion rate decreases but the fusion

dx.doi.org/10.1021/bi501159w | Biochemistry 2014, 53, 7184−7198

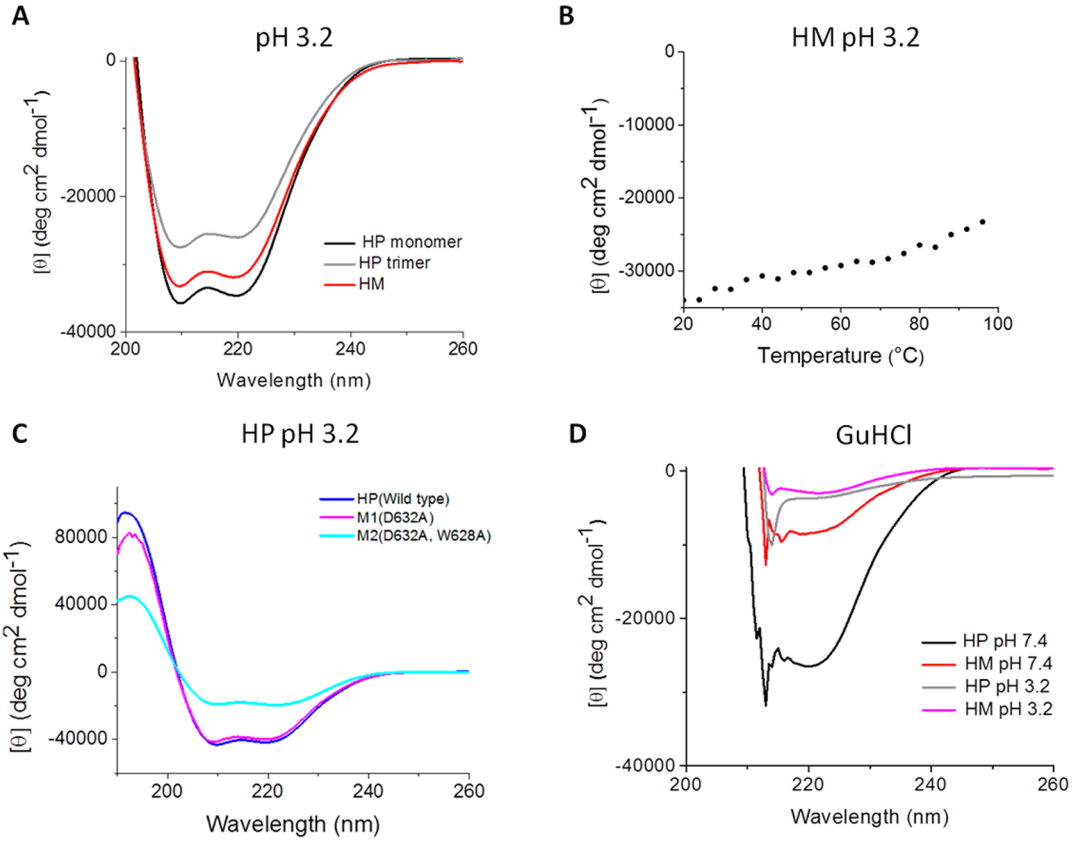

Figure 5. (A) CD spectra of HP and HM in pH 3.2 buffer. All spectra show θ_{222} indicative of a significant fraction of α helical structure. (B) θ_{222} vs temperature for HM at pH 3.2. No unfolding transition is observed. (C) CD spectra of WT and mutant HP at pH 3.2. For a SHB trimer, the D632A mutation could disrupt the intermonomer salt bridge with K574 and the W628A mutation could disrupt the intramonomer hydrophobic interaction with W571. More positive CD signal for the double but not the single mutant is consistent with monomer rather than SHB trimer HP at pH 3.2. (D) CD spectra of HP and HM in buffer with 6 M GuHCl. The spectra show θ_{222} indicative of a significant fraction of α helical structure. The [protein] $\approx$ 15 μM (~0.2 mg/mL), the pH 3.2 buffers contained 50 mM formate with 0.2 mM TCEP, and the pH 7.4 buffers contained 10 mM phosphate and 2 mM DTT.

extent increases where the latter effect is probably due to reduced intervesicle electrostatic repulsion.[42]

Fusion is enhanced with inclusion of the MPER in the construct as evidenced by the following differences for HM relative to HP with POPG vesicles: (1) at pH 3.2, higher initial fusion rate and (2) at pH 7.4, higher final fusion extent (M_f). For pH 3.2, the final [protein] = 0.2 μM (~0.003 mg/mL) and the hairpin monomer likely makes initial contact with the vesicle. HM-induced fusion occurs within a few seconds, so the monomer is likely a fusion-active species. The enhanced fusion with inclusion of the MPER is consistent with earlier observations of vesicle fusion induced by MPER peptides.

Synergy of FP, Hairpin, and MPER with the gp41 Copy Number of a Virion. The individual and collective contributions of the FP, hairpin, and MPER to ectodomain-induced fusion were studied with HP, HM, and FP-HM solubilized as hexamers in 6 M GuHCl. The final [GuHCl] = 40 mM and in the absence of protein, only modest fusion was observed at pH 3.2 ($M_f \approx 4\%$) and no fusion was observed at pH 7.4 (Supporting Information). Much greater fusion was observed with protein (Figure 7). Relative to HP which lacked most of the MPER, inclusion of the full MPER in HM resulted in higher M_f. Even greater M_f was induced for FP-HM which contains both the FP and MPER. Similar quantitative binding was observed in the absence and presence of the FP.[41,42] Dose response was observed for HM and FP-HM (Figure 8). A substantial M_f of ~15% was observed for FP-HM even at ultralow protein/lipid = 1:4800 that corresponds to ~15 proteins per ~100 nm diameter vesicle, estimated using the area-per-lipid. This number is significant because it is comparable to the ~30 gp41 molecules per virion. To our knowledge, this is the first observation of rapid (~5 s) ectodomain-mediated vesicle fusion at the protein copy number of a virion. In some contrast, rapid FP or MPER peptide-induced vesicle fusion has typically been observed at 500−1000 peptides per vesicle. Our result highlights the importance of the whole ectodomain in fusion, including contributions from FP, hairpin, and MPER regions.[43,44] The fusogenicity of FP-HM is even higher than shown in Figure 8 because our FP-HM stock contained ~40% HM impurity.

Although the stock protein is predominantly hexameric (Figure 4), the fusion-active oligomeric state is not clear because of the ~200-fold dilution of protein and GuHCl prior to fusion. HP is a monomer at equilibrium under these diluted conditions (Figure 3) and HM and FP-HM are probably monomers as well. Protein stock with 6 M GuHCl was used because this was the only condition for which FP-HM was soluble at ~1 mg/mL.

Folded Hairpin Ectodomain with MPER Binds bNAbs. The MPER region of gp41 includes the linear epitopes of several bNAbs and there is consequently continued effort to develop a MPER-based immunogen as a HIV vaccine. HM or

dx.doi.org/10.1021/bi501159w | Biochemistry 2014, 53, 7184−7198

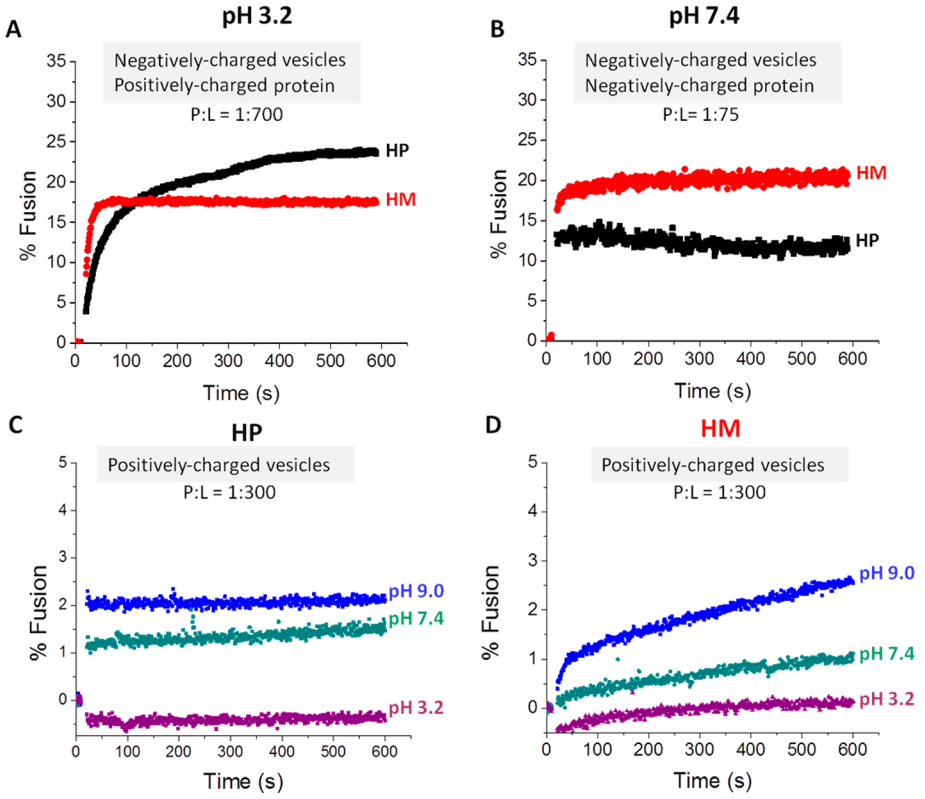

Figure 6. Vesicle fusion at 37 °C. Protein was added just prior to the increase in fusion with ~5 s assay dead time. For panels A and B, the vesicles were negatively charged and for panels C and D, the vesicles were positively charged. The calculated protein charge is +16, −2, and −4 at respective pH values 3.2, 7.4, and 9.0. The protein:lipid mole ratios were: (A) 1:700, (B) 1:75, and (C, D) 1:300, with Chol not included in the lipid quantity. The data overall support the importance of attractive protein/vesicle attractive energy for fusion at low protein:lipid ratios. The protein stock contained 20 μM protein (~0.25 mg/L) in 10 mM formate at pH 3.2 with 0.2 mM TCEP which are condition for predominant monomeric protein. For panels A and B, [POPC] = 120 μM, [POPG] = 30 μM, and [Chol] = 75 μM, and for panels C and D, the vesicles contained [POPC] = 120 μM, [DOTAP] = 30 μM, and [Chol] = 75 μM. Vesicle buffers were 10 mM formate at pH 3.2, 5 mM HEPES/10 mM MES at pH 7.4, and 10 mM Tris-HCl at pH 9.0.

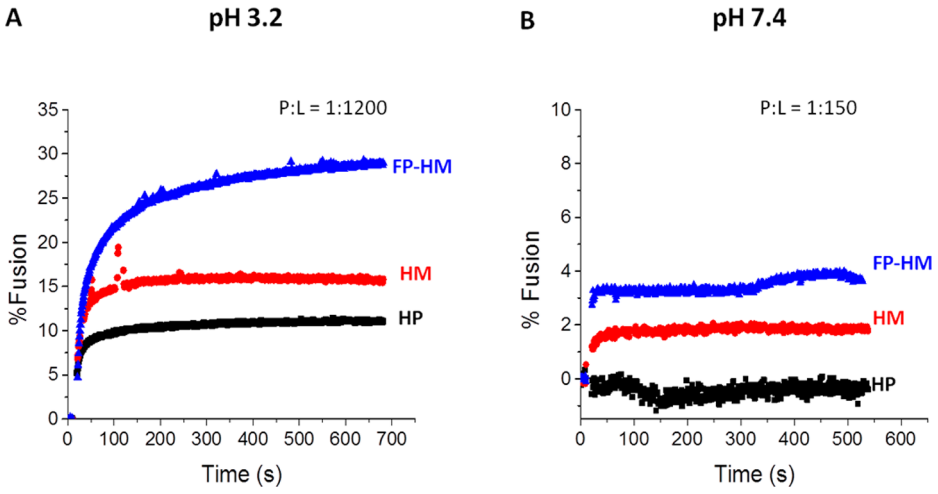

Figure 7. Vesicle fusion at 37 °C. A 7.5 μL aliquot of protein was added just prior to the increase in fusion and the final total volume was 1200 μL. The POPC/POPG/Chol vesicle composition and buffers were the same as Figure 6. The protein stock buffer was 10 mM formate at pH 3.2 with 6 M GuHCl and 0.2 mM TCEP and following addition of protein stock, the assay buffer contained 40 mM GuHCl. For the pH 3.2 assays, the stock [protein] = 20 μM (~0.25 mg/mL), and for the pH 7.4 assays, the stock [protein] = 160 μM (~2 mg/mL). The [protein]/[POPC + POPG] = 1:1200 for the pH 3.2 assays and 1:150 for the pH 7.4 assays.

similar folded hairpin molecules are appealing because of their high stability but there are conflicting data about the extent to which they bind bNAbs. However, our Western blots show reproducible binding of HM to the 4E10 bNAb (Figure 9A). HP lacks the 4E10 epitope and serves as a negative control. Western blots also show that HM binds to the 2F5 bNAb more strongly than HP which includes only part of the 2F5 epitope (Figures 9B and 1B). In the Western blot approach, the protein

dx.doi.org/10.1021/bi501159w | *Biochemistry* 2014, 53, 7184−7198

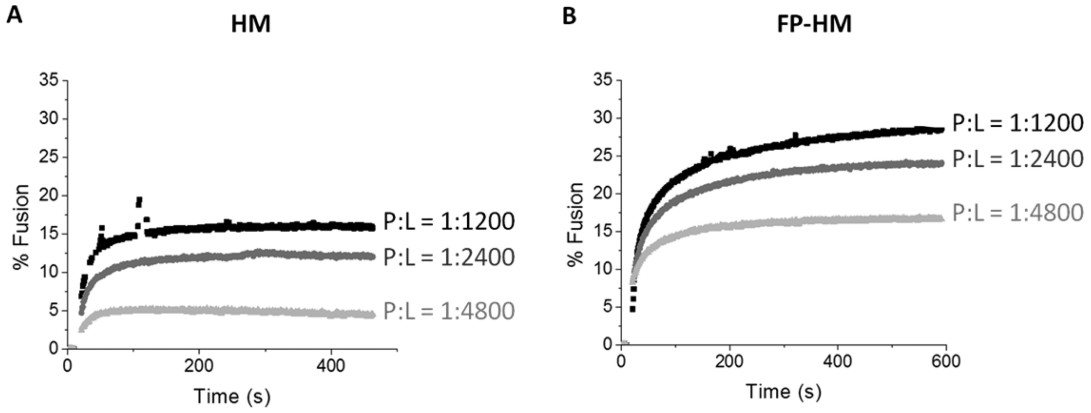

Figure 8. Dose response of vesicle fusion induced by HM and FP-HM at pH 3.2. The assay conditions were the same as Figure 7A except that the protein stock concentrations were 20, 10, and 5 μM for [protein]/[total lipid] = 1:1200, 1:2400, and 1:4800, respectively.

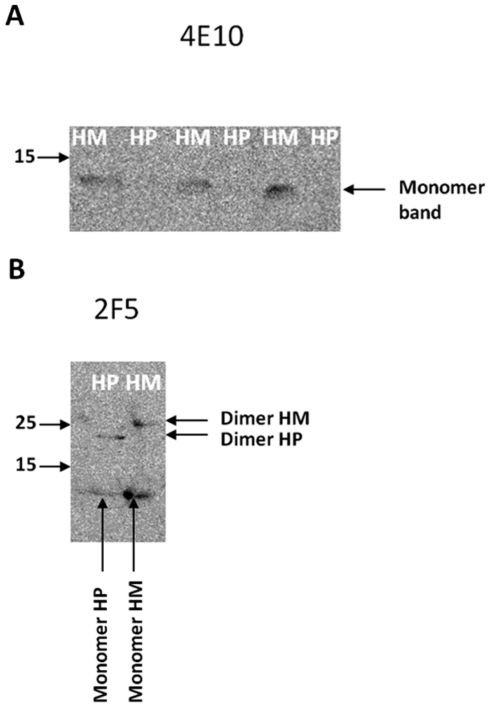

Figure 9. Western blots showing binding of HM to the 4E10 and 2F5 bNAbs and weaker binding of HP to 2F5. The left-side arrows are MWs in kDa.

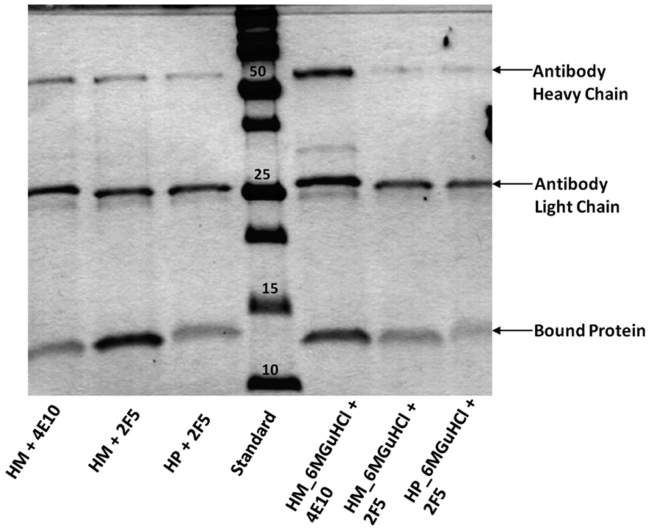

Figure 10. SDS-PAGE of the immunoprecipitation of HP and HM with the 4E10 and 2F5 bNAbs. There is stronger binding of HM to 4E10 and 2F5 and weaker binding of HP to 2F5. The protein stock buffer contained 50 mM sodium formate at pH 3.2 with 150 mM NaCl. For the right three lanes of the panel A gel, the buffer also contained 6 M GuHCl whereas for the left three lanes of panel A, the GuHCl was absent. Binding was done in PBS at pH 7.4 and for the right lanes, the diluted [GuHCl] = 10 mM. The center lane is the MW ladder in kDa.

is in 15% SDS prior to antibody binding. Although we do not know HM structure in this condition, HM hairpin structure is hyperthermostable and a shorter ectodomain construct without the MPER forms crystals in SDS with helical SHB structure.[45] A gel shift is not observed between HP and HM (Figures 2B and 9B) and could be the result of folded rather than random coil structure. HM is predominantly monomeric in 15% SDS and may therefore bind bNAb as a hairpin monomer. The blots also show minor dimer populations binding to 2F5.

Binding to bNAbs was probed under physiological conditions using direct immunoprecipitation. The protein stock solution contained either monomeric or hexameric protein and the binding was done at pH 7.4 with [GuHCl] < 10 mM. For either initial oligomeric state, HM bound to 4E10 and 2F5 (Figure 10) whereas there was no binding to IgG (Supporting Information). This is the antigenicity needed for a vaccine immunogen. HP binds 2F5 weaker than HM which is consistent with an incomplete epitope in HP.

DISCUSSION

Significant Findings. The ectodomain of the HIV gp41 protein plays a major role in catalyzing fusion between HIV and host cell membranes. The likely respective binding of the FP and MPER to the host cell and viral membranes are probably part of the underlying physical basis for catalysis. Although there has been significant functional and structural study of FP and MPER peptides, there have been just a few investigations of these regions as part of the larger ectodomain. The present work shows the significance of the FP, hairpin, and MPER regions for ectodomain-induced vesicle fusion including fusion with ~15 proteins per vesicle which is comparable to the gp41 copy number of the virion. For FP or MPER peptides, there has typically only been appreciable rapid vesicle fusion at 500–

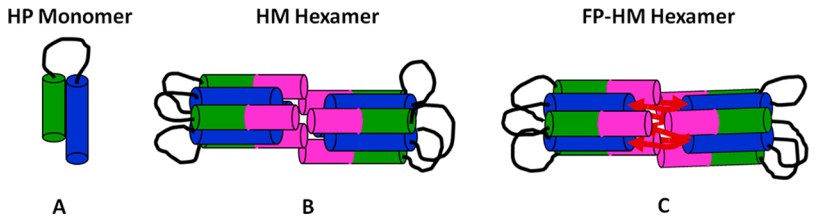

Figure 11. Working structural models of the gp41 ectodomain with Figure 1 color coding. Monomeric HP is modeled as the hairpin structure of a monomer in the SHB. HM and FP-HM hexamers are modeled as two SHB trimers that contact at their N-/C-terminal interfaces. This model correlates with the observed intermolecular antiparallel β sheet structure of FPs.

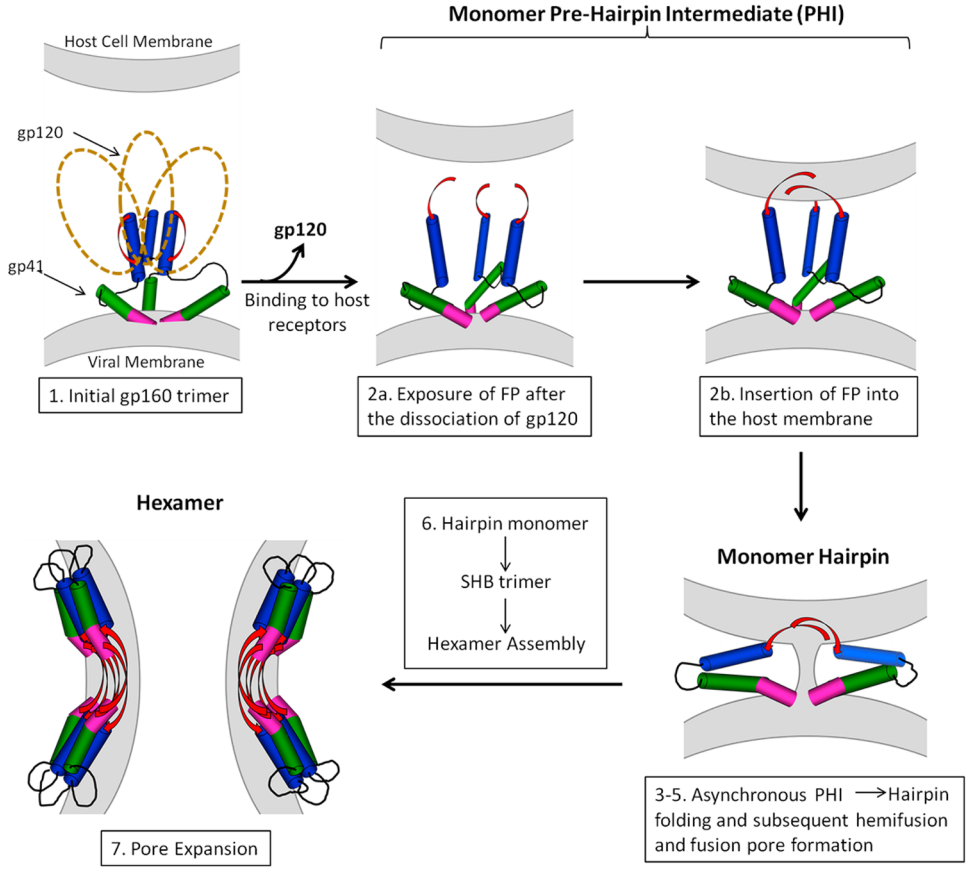

Figure 12. Model for membrane fusion that includes the gp41 ectodomain monomer and hexamer. The different regions of gp41 are color coded according to Figure 1 and the TM and endodomains are not shown. One of the monomers is not displayed in steps 3−5. The initial gp41 structure of step 1 is based on the ∼5 Å resolution gp140 structures and the final SHB structure of step 7 is based on high-resolution structures.

1000 peptides per vesicle and to our knowledge, ours is this first observation of rapid vesicle fusion at the virion gp41 copy number. Detection of either predominant monomer or hexamer gp41 ectodomain rather than trimer gp41 ectodomain was incorporated into the new HIV/host cell membrane fusion **model III** (Figure 12). One significant feature is inclusion of monomer ectodomain rather than trimer ectodomain PHI → hairpin folding at step 3. The free energy of gp41 ectodomain folding is coupled to free energy of formation of membrane intermediates. Our work may also aid HIV vaccine development via an immunogen with a folded gp41 ectodomain including MPER. This immunogen has the advantage of very high stability but there is literature disagreement about ectodomain binding to bNAbs. We show bNAb binding to gp41 ectodomain protein initially prepared as a monomer or hexamer.

SSNMR is a Novel and Important Tool in RP Production. One key result that moved the work forward was SSNMR detection of HM in IBs at ∼300 mg/L culture. The bottleneck to purified protein was therefore IB solubilization rather than expression and subsequent effort was focused on increasing solubilization. This result exemplifies how SSNMR is a general method to quantitate RP yield without solubilization or purification. High expression was obtained with common and inexpensive plasmids, *E. coli* strain, and growth and expression conditions. IB solubilization rather than expression may therefore be a general determinant of purified protein yield. Our yields were 15−50 mg/L and obtained with single-step affinity purification which should be advantageous in immunogen production. Our approach contrasts with earlier efforts that used protein fusion tags that had to be cleaved.[46]

dx.doi.org/10.1021/bi501159w | *Biochemistry* 2014, 53, 7184−7198

Monomer and Hexamer Rather than Trimer gp41 Ectodomain. For gp41 ectodomain constructs lacking solubility tags, only constructs with short NHR and CHR segments and no FP or MPER appear to form soluble trimers near pH 7.[47] For longer constructs that contain some or all of the FP or the MPER, for example, HP and HM, the present and earlier studies show most protein forming large aggregates (MW > 2 MDa) even in the presence of nonionic detergents.[48] There is solubility near pH 3 and many biophysical measurements have been done at this pH. High fractional helicity and T_m > 100 °C were considered strong evidence of SHB trimers.

One important contribution of the present study is SEC showing predominant monomer rather than trimer gp41 ectodomain at pH 3 (Figure 3). Our SEC monomer result is consistent with the SEC of large ectodomain constructs done by other groups (Figure 1A from ref 48 and Figure S1 from ref 51) although this monomer interpretation was typically not made by the authors of these papers. For these latter studies, the construct was NHR + native loop + CHR, FP + NHR + native loop + CHR + MPER + TM, or short NHR + short loop + short CHR.

The gp41 ectodomain monomer is highly helical and hyperthermostable. The most plausible monomer structure is *N*-helix/180° turn/C-helix model (Figure 11A) similar to the monomer unit of the high-resolution SHB trimer structures. The trimer is stabilized by several intermonomer NHR/NHR hydrophobic interactions and small reorientations of helices could reposition residues for favorable intramonomer NHR/CHR interactions. A looser helical monomer hairpin structure has been observed for a short NHR + loop + CHR construct in nonionic detergent but we favor the tight structure of Figure 11A.[49] Large ectodomain constructs like HP and HM have T_m > 100 °C either in the absence or presence of detergent and this high thermostability likely reflects substantial interhelical contact in the folded monomer. The looser structure of much shorter ectodomain constructs may be reflected in their typical $T_m \leq 70$ °C.

Measurements of large ectodomain constructs at low pH should be interpreted in the context of monomer protein. For example, the hyperthermostability detected by calorimetry and CD is likely a consequence of intramolecular NHR/CHR interaction rather than intermolecular NHR/NHR interaction. The stability of the ectodomain monomer would be consistent with an important role for the monomer in fusion, discussed in a subsequent section and presented in Figure 12. We also note that rapid vesicle fusion using stock protein at low pH is likely a consequence of membrane perturbation by hairpin monomer rather than SHB trimer. This includes fusion of negatively charged vesicles at pH 3.2 (Figure 6A) and positively charged vesicles at pH 7.4 and 9.0 (Figure 6C and D).

For 10 mg HP/mL SEC loading, there is a major monomer peak as well as minor trimer and oligomer/aggregate peaks (Figure 3B). The normalized values of monomer:trimer:larger oligomer integrations are 0.72:0.18:0.10. These correspond to [monomer] ≈ 60 μM and [trimer] ≈ 5 μM using the experimentally determined 10-fold dilution in SEC. For the association equilibrium, 3 monomer ↔ trimer, the derived $K_a \approx 2 \times 10^7 M^{-2}$, and corresponds to equal mass concentrations of monomer and trimer for total HP of ~9 mg/mL (~90 mg/mL loading in SEC). Earlier analytical ultracentrifugation (AUC) data have been analyzed to yield $K_a \approx 5 \times 11^{11}$ M^{-2}.[14,50,51] We do not understand the discrepancy between the SEC and AUC analyses.

Protein hexamers were observed in 6 M GuHCl at either pH 3.2 or 7.4 (Figure 5). The data show the hexamer as the fundamental unit of oligomerization rather than the trimer, for example, dodecamers were observed but not nonamers. A reasonable model for a hexamer is a dimer of SHB trimers with intertrimer contact between the MPERs (Figure 11B). This model is consistent with the observed helical structure in the hexamer and with T_m > 100 °C. This model is also consistent with some of the crystal packing of SHB trimers.[39] In addition, SSNMR studies of FP structure in the membrane-associated gp41 ectodomain show an oligomeric FP β sheet with antiparallel but not parallel arrangement of the FP strands.[24] The antiparallel arrangement would be consistent with end-on arrangement of two SHB trimers (Figure 11C).

It is important to consider the impact that GuHCl may have on the ectodomain structure as GuHCl often but not always denatures proteins.[52] We think denaturation is unlikely for the ectodomain because there is substantial helical structure and T_m > 100 °C. In addition, to our knowledge, it is very unusual that denatured protein would have a well-defined oligomeric state other than monomer. The hexamer is also the dominant oligomeric state of a modified ectodomain construct in physiologic solution, that is, pH 7.4 without any GuHCl.[38] This Soc-gp41ectoM-Fd construct includes a central gp41ectoM region, which is very similar to FP-HM, as well as a ~9 kDa non-native Soc protein N-terminal of the FP and a ~2 kDa Fd non-native protein C-terminal of the MPER. The Soc and Fd proteins were chosen because they form homotrimers in physiological solution. However, there was only minor trimer population of Soc-gp41ectoM-Fd in physiologic solution. Instead, the hexamer was dominant with additional smaller populations of two larger oligomers. The overall oligomer distribution of Soc-gp41ectoM-Fd in physiologic solution is very similar to that of HP and HM in 6 M GuHCl with dominant hexamer and two minor higher-order oligomers that are reasonably assigned to dodecamer and 24-mer. It is likely that there are similar hexamer structures of HP, HM, and Soc-gp41ectoM-Fd.

Biophysical Model of Oligomerization. At neutral pH, large ectodomain constructs form >2 MDa aggregates, whereas at low pH, monomers predominate for <10 mg protein/mL and there is significant trimer population with SHB structure for >50 mg protein/mL. The pH-dependence of oligomeric state is observed with or without nonionic detergent so our explanatory model is based on relative magnitudes of protein electrostatic vs hydrophobic effects. Trimer stabilization is primarily because of hydrophobic interaction between the three NHR helices on the SHB interior. At low pH, there is a calculated charge of ~+10 for the hairpin region of the ectodomain monomer. We posit that monomer rather than oligomers are favored at low pH because intermolecular electrostatic repulsion overwhelms the hydrophobic interaction. At neutral pH, the calculated charge is −2 and hydrophobic interaction is dominant. The resulting aggregates may be composed of SHB trimers.

For solutions containing GuHCl at both low and neutral pH, hexamers predominate, that is, addition of GuHCl induces monomer → hexamer oligomerization at low pH and induces aggregate → hexamer breakup at neutral pH. To our knowledge, the specific interaction of positively charged GuH^+ with protein molecules is not understood.[53] For the

ectodomain protein, we posit that the hexamer is formed from two SHB trimers (Figure 11B and C) and that GuH^+ interacts with COO^- groups on the SHB surfaces. The $-COO^-$ rather than the $-COOH$ state is favored at both pH's because of attractive interaction with GuH^+. At low pH, this reduces the positive charge of the protein so that the SHB trimer does not dissociate due to electrostatic repulsion between monomers. Hexamers form because of favorable hydrophobic interaction between the FP/MPER end of one SHB trimer and the FP/MPER end of a second trimer. Aggregation beyond hexamers is disfavored because this aggregation would reduce exposed protein surface area and therefore the number of GuH^+/COO^- contacts. As noted above, SOC-gp41ectoM-Fd forms a hexamer in the absence of GuHCl, and we posit this is also two SHB trimers. Further aggregation is disfavored because of the solubility of the SOC and FD proteins and perhaps because of their steric bulk.

Correlation of Vesicle Fusion with HIV/Cell Fusion. One significant result is observation of vesicle fusion for ~15 FP-HM per vesicle (Figure 8B), which is comparable to the gp41 copy number of ~30 in the virion. To our knowledge, FP-HM thus provides the first example for which protein-induced vesicle fusion might reasonably be directly compared to viral fusion. FP-HM is more fusogenic than shorter ectodomain constructs like HP, which lacks the FP and MPER, and also more fusogenic than isolated FP or MPER peptides. This potent fusogenicity highlights the importance of the full ectodomain in fusion, with inclusion of the N-terminal FP, hairpin region, and C-terminal MPER. During HIV/cell fusion, the FP and MPER likely bind to the cell and HIV membranes, respectively, and higher fusion for FP-HM relative to HM supports synergy between these two regions, likely via membrane perturbations. Vesicle fusion is probably a better model of the earlier hemifusion (lipid mixing) step of viral fusion than the final fusion pore expansion step. Pore formation and expansion in vesicle fusion is less regulated than in HIV/cell fusion and leakage of contents out of the vesicles occurs much faster than mixing of contents between vesicles.

For conditions with attractive protein/vesicle electrostatic energy, protein/vesicle binding is quantitative and FP-independent. The observed FP-dependent fusogenicity is therefore not reasonably ascribed to FP-dependent binding. Protein binding is described by the equation $f_m = (K_m \times [L])/\{1 + (K_m \times [L])\}$ where f_m = fraction bound-protein, K_m = equilibrium constant derived from G_m = binding free-energy, and L = lipid. For our assays, $[L] = 1.5 \times 10^{-4}$ M and protein/vesicle binding is quantitative ($f_m = 1.0$) when $K_m > 10^5$ M^{-1}. The $G_m = G_{elec} + G_{hydro}$ and corresponding $K_m = K_{elec} \times K_{hydro}$ describe contributions from electrostatic and hydrophobic interactions. The FP is hydrophobic but lacks ionizable residues so it affects G_{hydro} but not G_{elec}. For negatively charged vesicles at pH 3 and positively charged vesicles at pH 9, the calculated $K_{elec} > 10^5$ M^{-1} and corresponds to quantitative binding of all proteins, which has also been experimentally observed. For conditions with much smaller K_{elec}, such as negatively charged vesicles at neutral pH, binding may be FP-dependent and changes in fusogenicity could be related to binding differences.

High fusion by FP-HM requires a pH for which there is attractive protein/vesicle electrostatic energy with resultant quantitative binding to the vesicles (Figure 6). Attractive electrostatic energy is not a requirement for fusion by the ectodomain of full-length gp41 in the virion, likely because the ectodomain is restricted to the space between the viral and host cell membranes. This spatial confinement favors protein binding to the membranes even without electrostatic attraction.

For the present study, a 0.2 fraction charged lipid was used which is larger than the typical fraction in the cell membrane. However, a recent study showed efficient vesicle fusion with much smaller fractions charged lipid.[42] As the fraction charged lipid is decreased, there is a corresponding increase in fusion extent that is likely due to decreased intervesicle electrostatic repulsion. Some charged lipid is needed for quantitative protein binding to the vesicles and consequently fusion. As one example, HP at protein/lipid = 1:700 (~100 HP molecules/vesicle) induced ~40% fusion of vesicles containing only 0.02 fraction negatively charged phosphatidylserine lipid. These results, along with the higher fusogenicity of FP-HM relative to HP (Figure 7A), support correlation between FP-HM induced vesicle fusion and hemifusion between the HIV and cell membranes mediated by the viral ectodomain. Viral fusion is probably also affected by membrane curvature and fluidity.

New Fusion Model with gp41 Monomer and Hexamer Ectodomain. As noted in the Introduction, models for gp160-induced membrane fusion have typically considered changes in structure of a gp160 trimer that are temporally and energetically coupled to changes in the topologies of the HIV and host cell membranes. **Models I** and **II** of the Introduction share the feature of trimeric ectodomain gp41 throughout fusion. For **model I**, concerted PHI → SHB trimer folding is coupled to subsequent hemifusion. However, this is inconsistent with fusion inhibition by CHR+MPER peptides up to the final pore expansion step and the corollary assumption of peptide binding to the PHI trimer but not the SHB trimer. **Model II** delays the PHI → SHB trimer folding until the pore expansion step which suggests that the SHB is only associated with fused membrane stabilization and fusion arrest. The new **model III** incorporates asynchronous ectodomain monomer PHI → hairpin folding followed by changes in membrane topology leading to hemifusion (Figure 12). There is subsequent ectodomain monomer hairpin assembly into SHB trimers and final assembly of two trimers into a hexamer with an antiparallel FP β sheet like Figure 11 C model. During viral fusion, the N-terminal FP is likely attached to the cell membrane and the *C*-terminal TM is in the viral membrane. In our view, these membrane topologies are more reasonably maintained with asynchronous folding of individual monomer ectodomains than with concerted folding of the three ectodomains of the trimer. Asynchronous ectodomain monomer folding to a hairpin is also consistent with the hyperthermostability ($T_m \approx 110$ °C) of the monomer hairpin. **Model III** is based on integration of findings of the present study including ectodomain monomers and hexamers with previous biophysical and viral fusion results.

There is evidence supporting the involvement of monomer hairpin gp41 ectodomain at some stage of HIV/host cell fusion. Such fusion has typically been assayed using the surrogate system of fusion between cells expressing gp160 and cells expressing CD4 and coreceptor proteins. Fusion is quantitated using the number of syncytia (fused cell aggregates). There is typically dramatic reduction in fusion with mutations impacting intramonomer CHR/NHR interactions, for example, no syncytia are formed with the W571R mutation.[54] Membrane fusion and HIV infection are inhibited by the clinically prescribed CHR + MPER enfuvirtide therapeutic which could act by binding to exposed NHR surfaces in the PHI or hairpin ectodomain monomer but would not bind to the SHB trimer for which the three NHR helices are on the bundle interior.[55]

dx.doi.org/10.1021/bi501159w | *Biochemistry* 2014, 53, 7184−7198

The physiological relevance of the gp41 ectodomain monomer is also supported by observation of monomer rather than trimer WT gp140 protein.[8] Gp140 is a noncovalent complex between the HIV gp120 protein and the ectodomain of gp41 but lacks the TM and intraviral regions of gp41.

A role for hexameric gp41 in HIV/cell fusion is supported by the trans-dominant effect of the V513E mutation in the FP region of gp41 on gp160-mediated membrane fusion and HIV infection.[56] These data have been modeled using a requirement of multiple gp160 trimers for fusion and infection.[26] A membrane-associated gp41 hexamer is consistent with the antiparallel β sheet FP structure in the membrane-associated gp41 ectodomain observed by SSNMR.[24] Such structure is consistent with interleaved FP strands from two trimers (Figure 11C).

In the course of publishing this work, another paper was published showing that a shorter NHR + loop + CHR gp41 ectodomain construct is monomeric at low pH in nonionic detergent.[49] This result is consistent with our observations for the larger HP and HM constructs. We also observed that pH rather than detergent is the critical parameter for solubility. In the absence of GuHCl, both the HP and HM constructs are soluble at low pH and insoluble at neutral pH and these results are independent of the presence or absence of detergent. The short construct in detergent at low pH has a loose hairpin structure with noninteracting NHR and CHR helices which lie on the micelle surface. The low pH micelle location is consistent with our observations of protein-to-lipid headgroup contact for a large, membrane-associated ectodomain construct. At low pH, NHR+CHR backbone ^{13}CO-to-lipid ^{31}P distances of 8−9 Å were observed via SSNMR spectroscopy.[42] At neutral pH, there was no detectable contact which corresponds to ^{13}CO−^{31}P distances >12 Å even though the protein remained membrane-bound via the FP region. The pH-dependence of the protein-to-lipid distances is consistent with the attractive protein/membrane electrostatic energy at low pH and repulsive energy at neutral pH.

Although not included in the gp41 constructs of the present study, the TM domain is important for anchoring gp41 in the viral membrane and is likely also important in fusion pore formation.[57] The TM sequence is conserved across clades of HIV and this conservation may be needed for efficient trafficking of gp160 to the infected cell membrane surface prior to viral budding.[58] There are moderate effects on fusion and infection with some mutations in the TM region.[59,60] It would be interesting in the future to study the oligomerization and fusion activity of gp41 constructs that include the TM domain. SEC of a full ectodomain + TM construct showed predominant monomers at pH 4 in detergent which is consistent with the SEC for ectodomain without TM.[51] There was little contact between the FP and TM regions for the large construct in detergent but some contact has been observed between synthesized FP peptide and TM peptide in membranes.[61]

■ ASSOCIATED CONTENT

Supporting Information

Material suppliers, DNA sequence of HM insert, and additional RP-HPLC, SEC, mass spectra, and immunoprecipitation data. This material is available free of charge via the Internet at http://pubs.acs.org.

■ AUTHOR INFORMATION

Corresponding Author

*Phone: 517-355-9715. Fax: 517-353-1793. E-mail: weliky@chemistry.msu.edu.

Funding

The research was supported by the National Institutes of Health grant A147153.

Notes

The authors declare no competing financial interest.

■ ACKNOWLEDGMENTS

The following reagent was obtained through the NIH AIDS Research and Reference Reagent Program, Division of AIDS, NIAID, NIH: HIV-1 gp41 Monoclonal Antibodies (4E10 and 2F5) from Dr. Hermann Katinger. We acknowledge Matthew J. Nethercott for assistance with CD spectroscopy.

■ ABBREVIATIONS

AUC = analytical ultracentrifugation; BCA = bicinchoninic assay; bNAb = broadly neutralizing antibody; CD = circular dichroism; Chol = cholesterol; CHR = C-terminal heptad repeat; DOTAP = 1,2-dioleoyl-3-trimethylammonium-propane (chloride salt); FP = fusion peptide; gp140 = gp120+gp41 ectodomain; gp160 = gp120+gp41; GuHCl = guanidine hydrochloride; IB = inclusion body; HEPES = 4-(2-hydroxyethyl)-1-piperazineethanesulfonic acid; IPTG = isopropyl β-D-1-thiogalactopyranoside; LB = Luria−Bertani; MES = 2-(*N*-morpholino)ethanesulfonic acid; MPAA = *S*-trityl-β-mercaptopropionic acid; MPER = membrane-proximal external region; SHB = six-helix bundle; NHR = N-terminal heptad repeat; *N*-NBD-DPPE = *N*-(7-nitro-2,1,3-benzoxadiazol-4-yl) (ammonium salt) dipalmitoylphosphatidylethanolamine; *N*-Rh-DPPE = *N*-(lissamine rhodamine B sulfonyl) (ammonium salt) dipalmitoylphosphatidylethanolamine; PHI = prehairpin intermediate; POPC = 1-palmitoyl-2-oleoyl-*sn*-glycero-3-phosphocholine; POPG = 1-palmitoyl-2-oleoyl-*sn*-glycero-3-[phospho-rac-(1-glycerol)] (sodium salt); RP = recombinant protein; RP-HPLC = reversed-phase HPLC; SEC = size-exclusion chromatography; SSNMR = solid-state nuclear magnetic resonance; TCEP = tris(2-carboxyethyl) phosphine hydrochloride

■ REFERENCES

(1) Grewe, C., Beck, A., and Gelderblom, H. R. (1990) HIV: Early virus-cell interactions. *J. AIDS 3*, 965−974.

(2) White, J. M., Delos, S. E., Brecher, M., and Schornberg, K. (2008) Structures and mechanisms of viral membrane fusion proteins: Multiple variations on a common theme. *Crit. Rev. Biochem. Mol. Biol. 43*, 189−219.

(3) Melikyan, G. B. (2014) HIV entry: a game of hide-and-fuse? *Curr. Opin. Virol. 4*, 1−7.

(4) Durell, S. R., Martin, I., Ruysschaert, J. M., Shai, Y., and Blumenthal, R. (1997) What studies of fusion peptides tell us about viral envelope glycoprotein-mediated membrane fusion. *Mol. Membr. Biol. 14*, 97−112.

(5) Montero, M., van Houten, N. E., Wang, X., and Seott, J. K. (2008) The membrane-proximal external region of the human immunodeficiency virus type 1 envelope: Dominant site of antibody neutralization and target for vaccine design. *Microbiol. Mol. Biol. Rev. 72*, 54−84.

(6) Apellaniz, B., Huarte, N., Largo, E., and Nieva, J. L. (2014) The three lives of viral fusion peptides. *Chem. Phys. Lipids 181*, 40−55.

(7) Liu, J., Bartesaghi, A., Borgnia, M. J., Sapiro, G., and Subramaniam, S. (2008) Molecular architecture of native HIV-1 gp120 trimers. *Nature 455*, 109−113.
(8) Schulke, N., Vesanen, M. S., Sanders, R. W., Zhu, P., Lu, M., Anselma, D. J., Villa, A. R., Parren, P., Binley, J. M., Roux, K. H., Maddon, P. J., Moore, J. P., and Olson, W. C. (2002) Oligomeric and conformational properties of a proteolytically mature, disulfide-stabilized human immunodeficiency virus type 1 gp140 envelope glycoprotein. *J. Virol. 76*, 7760−7776.
(9) Sanders, R. W., Vesanen, M., Schuelke, N., Master, A., Schiffner, L., Kalyanaraman, R., Paluch, M., Berkhout, B., Maddon, P. J., Olson, W. C., Lu, M., and Moore, J. P. (2002) Stabilization of the soluble, cleaved, trimeric form of the envelope glycoprotein complex of human immunodeficiency virus type 1. *J. Virol. 76*, 8875−8889.
(10) Bartesaghi, A., Merk, A., Borgnia, M. J., Milne, J. L. S., and Subramaniam, S. (2013) Prefusion structure of trimeric HIV-1 envelope glycoprotein determined by cryo-electron microscopy. *Nat. Struct. Mol. Biol. 20*, 1352−1357.
(11) Julien, J.-P., Cupo, A., Sok, D., Stanfield, R. L., Lyumukis, D., Deller, M. C., Klasse, P.-J., Burton, D. R., Sanders, R. W., Moore, J. P., Ward, A. B., and Wilson, I. A. (2013) Crystal structure of a soluble cleaved HIV-1 envelope trimer. *Science 342*, 1477−1483.
(12) Lyumukis, D., Julien, J.-P., de Val, N., Cupo, A., Potter, C. S., Klasse, P.-J., Burton, D. R., Sanders, R. W., Moore, J. P., Carragher, B., Wilson, I. A., and Ward, A. B. (2013) Cryo-EM structure of a fully glycosylated soluble cleaved HIV-1 envelope trimer. *Science 342*, 1484−1490.
(13) Tan, K., Liu, J., Wang, J., Shen, S., and Lu, M. (1997) Atomic structure of a thermostable subdomain of HIV-1 gp41. *Proc. Natl. Acad. Sci. U.S.A. 94*, 12303−12308.
(14) Caffrey, M., Cai, M., Kaufman, J., Stahl, S. J., Wingfield, P. T., Covell, D. G., Gronenborn, A. M., and Clore, G. M. (1998) Three-dimensional solution structure of the 44 kDa ectodomain of SIV gp41. *EMBO J. 17*, 4572−4584.
(15) Yang, Z. N., Mueser, T. C., Kaufman, J., Stahl, S. J., Wingfield, P. T., and Hyde, C. C. (1999) The crystal structure of the SIV gp41 ectodomain at 1.47 A resolution. *J. Struct. Biol. 126*, 131−144.
(16) Buzon, V., Natrajan, G., Schibli, D., Campelo, F., Kozlov, M. M., and Weissenhorn, W. (2010) Crystal structure of HIV-1 gp41 including both fusion peptide and membrane proximal external regions. *PLoS Pathog. 6*, No. e1000880.
(17) Lu, M., Ji, H., and Shen, S. (1999) Subdomain folding and biological activity of the core structure from human immunodeficiency virus type 1 gp41: implications for viral membrane fusion. *J. Virol. 73*, 4433−4438.
(18) Sackett, K., Nethercott, M. J., Epand, R. F., Epand, R. M., Kindra, D. R., Shai, Y., and Weliky, D. P. (2010) Comparative analysis of membrane-associated fusion peptide secondary structure and lipid mixing function of HIV gp41 constructs that model the early pre-hairpin intermediate and final hairpin conformations. *J. Mol. Biol. 397*, 301−315.
(19) Wild, C. T., Shugars, D. C., Greenwell, T. K., McDanal, C. B., and Matthews, T. J. (1994) Peptides corresponding to a predictive alpha-helical domain of human immunodeficiency virus type 1 gp41 are potent inhibitors of virus infection. *Proc. Natl. Acad. Sci. U.S.A. 91*, 9770−9774.
(20) Markosyan, R. M., Cohen, F. S., and Melikyan, G. B. (2003) HIV-1 envelope proteins complete their folding into six-helix bundles immediately after fusion pore formation. *Mol. Biol. Cell 14*, 926−938.
(21) Matthews, T., Salgo, M., Greenberg, M., Chung, J., DeMasi, R., and Bolognesi, D. (2004) Enfuvirtide: The first therapy to inhibit the entry of HIV-1 into host CD4 lymphocytes. *Nat. Rev. Drug Discovery 3*, 215−225.
(22) Chernomordik, L. V., and Kozlov, M. M. (2008) Mechanics of membrane fusion. *Nat. Struct. Mol. Biol. 15*, 675−683.
(23) Weissenhorn, W., Dessen, A., Harrison, S. C., Skehel, J. J., and Wiley, D. C. (1997) Atomic structure of the ectodomain from HIV-1 gp41. *Nature 387*, 426−430.
(24) Sackett, K., Nethercott, M. J., Zheng, Z. X., and Weliky, D. P. (2014) Solid-state NMR spectroscopy of the HIV gp41 membrane fusion protein supports intermolecular antiparallel beta sheet fusion peptide structure in the final six-helix bundle state. *J. Mol. Biol. 426*, 1077−1094.
(25) Sougrat, R., Bartesaghi, A., Lifson, J. D., Bennett, A. E., Bess, J. W., Zabransky, D. J., and Subramaniam, S. (2007) Electron tomography of the contact between T cells and SIV/HIV-1: Implications for viral entry. *PLoS Pathogens 3*, 570−581.
(26) Magnus, C., Rusert, P., Bonhoeffer, S., Trkola, A., and Regoes, R. R. (2009) Estimating the stoichiometry of Human Immunodeficiency Virus entry. *J. Virol. 83*, 1523−1531.
(27) Yang, J., Prorok, M., Castellino, F. J., and Weliky, D. P. (2004) Oligomeric b-structure of the membrane-bound HIV-1 fusion peptide formed from soluble monomers. *Biophys. J. 87*, 1951−1963.
(28) Shnaper, S., Sackett, K., Gallo, S. A., Blumenthal, R., and Shai, Y. (2004) The C- and the N-terminal regions of glycoprotein 41 ectodomain fuse membranes enriched and not enriched with cholesterol, respectively. *J. Biol. Chem. 279*, 18526−18534.
(29) Apellaniz, B., Garcia-Saez, A. J., Nir, S., and Nieva, J. L. (2011) Destabilization exerted by peptides derived from the membrane-proximal external region of HIV-1 gp41 in lipid vesicles supporting fluid phase coexistence. *Biochim. Biophys. Acta 1808*, 1797−1805.
(30) Zhu, P., Chertova, E., Bess, J., Lifson, J. D., Arthur, L. O., Liu, J., Taylor, K. A., and Roux, K. H. (2003) Electron tomography analysis of envelope glycoprotein trimers on HIV and simian immunodeficiency virus virions. *Proc. Natl. Acad. Sci. U.S.A. 100*, 15812−15817.
(31) Huang, J. H., Ofek, G., Laub, L., Louder, M. K., Doria-Rose, N. A., Longo, N. S., Imamichi, H., Bailer, R. T., Chakrabarti, B., Sharma, S. K., Alam, S. M., Wang, T., Yang, Y. P., Zhang, B. S., Migueles, S. A., Wyatt, R., Haynes, B. F., Kwong, P. D., Mascola, J. R., and Connors, M. (2012) Broad and potent neutralization of HIV-1 by a gp41-specific human antibody. *Nature 491*, 406−412.
(32) Frey, G., Peng, H., Rits-Volloch, S., Morelli, M., Cheng, Y., and Chen, B. (2008) A fusion-intermediate state of HIV-1 gp41 targeted by broadly neutralizing antibodies. *Proc. Natl. Acad. Sci. U.S.A. 105*, 3739−3744.
(33) Wang, J., Tong, P., Lu, L., Zhou, L. L., Xu, L. L., Jiang, S. B., and Chen, Y. H. (2011) HIV-1 gp41 core with exposed membrane-proximal external region inducing broad HIV-1 neutralizing antibodies. *PLoS One 6*, e18233.
(34) Dawood, R., Benjelloun, F., Pin, J. J., Kone, A., Chanut, B., Jospin, F., Lucht, F., Verrier, B., Moog, C., Genin, C., and Paul, S. (2013) Generation of HIV-1 potent and broad neutralizing antibodies by immunization with postfusion HR1/HR2 complex. *AIDS 27*, 717−730.
(35) Sackett, K., Nethercott, M. J., Shai, Y., and Weliky, D. P. (2009) Hairpin folding of HIV gp41 abrogates lipid mixing function at physiologic pH and inhibits lipid mixing by exposed gp41 constructs. *Biochemistry 48*, 2714−2722.
(36) Vogel, E. P., and Weliky, D. P. (2013) Quantitation of recombinant protein in whole cells and cell extracts via solid-state NMR spectroscopy. *Biochemistry 52*, 4285−4287.
(37) Lev, N., Fridmann-Sirkis, Y., Blank, L., Bitler, A., Epand, R. F., Epand, R. M., and Shai, Y. (2009) Conformational stability and membrane interaction of the full-length ectodomain of HIV-1 gp41: Implication for mode of action. *Biochemistry 48*, 3166−3175.
(38) Gao, G. F., Wieczorek, L., Peachman, K. K., Polonis, V. R., Alving, C. R., Rao, M., and Rao, V. B. (2013) Designing a soluble near full-length HIV-1 gp41 trimer. *J. Biol. Chem. 288*, 234−246.
(39) Shi, W. X., Bohon, J., Han, D. P., Habte, H., Qin, Y. L., Cho, M. W., and Chance, M. R. (2010) Structural characterization of HIV gp41 with the membrane-proximal external region. *J. Biol. Chem. 285*, 24290−24298.
(40) Brugger, B., Glass, B., Haberkant, P., Leibrecht, I., Wieland, F. T., and Krasslich, H. G. (2006) The HIV lipidome: A raft with an unusual composition. *Proc. Natl. Acad. Sci. U.S.A. 103*, 2641−2646.
(41) Sackett, K., TerBush, A., and Weliky, D. P. (2011) HIV gp41 six-helix bundle constructs induce rapid vesicle fusion at pH 3.5 and

little fusion at pH 7.0: understanding pH dependence of protein aggregation, membrane binding, and electrostatics, and implications for HIV-host cell fusion. *Eur. Biophys. J. 40*, 489−502.
(42) Ratnayake, P., Sackett, K., Nethercott, M. J., Weliky, D. P. pH-dependent vesicle fusion induced by the ectodomain of the Human Immunodeficiency Virus membrane fusion protein gp41: Two kinetically distinct processes and fully-membrane-associated gp41 with predominant beta sheet fusion peptide conformation, *Biochim. Biophys. Acta*, in press.
(43) Suarez, T., Gallaher, W. R., Agirre, A., Goni, F. M., and Nieva, J. L. (2000) Membrane interface-interacting sequences within the ectodomain of the human immunodeficiency virus type 1 envelope glycoprotein: Putative role during viral fusion. *J. Virol. 74*, 8038−8047.
(44) Kim, C. S., Epand, R. F., Leikina, E., Epand, R. M., and Chernomordik, L. V. (2011) The final conformation of the complete ectodomain of the HA2 subunit of Influenza Hemagglutinin can by itself drive low pH-dependent fusion. *J. Biol. Chem. 286*, 13226−13234.
(45) Shu, W., Ji, H., and Lu, M. (2000) Interactions between HIV-1 gp41 core and detergents and their implications for membrane fusion. *J. Biol. Chem. 275*, 1839−1845.
(46) Lin, C. H., Lin, C. H., Chang, C. C., Wei, T. S., Cheng, S. F., Chen, S. S. L., and Chang, D. K. (2011) An efficient production and characterization of HIV-1 gp41 ectodomain with fusion peptide in Escherichia coli system. *J. Biotechnol. 153*, 48−55.
(47) Shu, W., Liu, J., Ji, H., Radigen, L., Jiang, S. B., and Lu, M. (2000) Helical interactions in the HIV-1 gp41 core reveal structural basis for the inhibitory activity of gp41 peptides. *Biochemistry 39*, 1634−1642.
(48) Caffrey, M., Braddock, D. T., Louis, J. M., Abu-Asab, M. A., Kingma, D., Liotta, L., Tsokos, M., Tresser, N., Pannell, L. K., Watts, N., Steven, A. C., Simon, M. N., Stahl, S. J., Wingfield, P. T., and Clore, G. M. (2000) Biophysical characterization of gp41 aggregates suggests a model for the molecular mechanism of HIV-associated neurological damage and dementia. *J. Biol. Chem. 275*, 19877−19882.
(49) Roche, J., Louis, J. M., Grishaev, A., Ying, J. F., and Bax, A. (2014) Dissociation of the trimeric gp41 ectodomain at the lipid-water interface suggests an active role in HIV-1 Env-mediated membrane fusion. *Proc. Natl. Acad. Sci. U.S.A. 111*, 3425−3430.
(50) Caffrey, M., Kaufman, J., Stahl, S., Wingfield, P., Gronenborn, A. M., and Clore, G. M. (1999) Monomer-trimer equilibrium of the ectodomain of SIV gp41: Insight into the mechanism of peptide inhibition of HIV infection. *Protein Sci. 8*, 1904−1907.
(51) Lakomek, N. A., Kaufman, J. D., Stahl, S. J., Louis, J. M., Grishaev, A., Wingfield, P. T., and Bax, A. (2013) Internal dynamics of the homotrimeric HIV-1 viral coat protein gp41 on multiple time scales. *Angew. Chem., Int. Ed. 52*, 3911−3915.
(52) Moon, C. P., Kwon, S., and Fleming, K. G. (2011) Overcoming hysteresis to attain reversible equilibrium folding for outer membrane phospholipase A in phospholipid bilayers. *J. Mol. Biol. 413*, 484−494.
(53) Lim, W. K., Rosgen, J., and Englander, S. W. (2009) Urea, but not guanidinium, destabilizes proteins by forming hydrogen bonds to the peptide group. *Proc. Natl. Acad. Sci. U.S.A. 106*, 2595−2600.
(54) Cao, J., Bergeron, L., Helseth, E., Thali, M., Repke, H., and Sodroski, J. (1993) Effects of amino-acid changes in the extracellular comain of the Human Immunodeficiency Virus Type-1 gp41 envelope glycoprotein. *J. Virol. 67*, 2747−2755.
(55) Peisajovich, S. G., and Shai, Y. (2001) SIV gp41 binds to membranes both in the monomeric and trimeric states: Consequences for the neuropathology and inhibition of HIV infection. *J. Mol. Biol. 311*, 249−254.
(56) Freed, E. O., Delwart, E. L., Buchschacher, G. L., Jr., and Panganiban, A. T. (1992) A mutation in the human immunodeficiency virus type 1 transmembrane glycoprotein gp41 dominantly interferes with fusion and infectivity. *Proc. Natl. Acad. Sci. U.S.A. 89*, 70−74.
(57) Kemble, G. W., Danieli, T., and White, J. M. (1994) Lipid-anchored influenza hemagglutinin promotes hemifusion, not complete fusion. *Cell 76*, 383−391.
(58) Miyauchi, K., Curran, A. R., Long, Y. F., Kondo, N., Iwamoto, A., Engelman, D. M., and Matsuda, Z. (2010) The membrane-spanning domain of gp41 plays a critical role in intracellular trafficking of the HIV envelope protein. *Retrovirology 7*, 95.
(59) Wilk, T., Pfeiffer, T., Bukovsky, A., Moldenhauer, G., and Bosch, V. (1996) Glycoprotein incorporation and HIV-1 infectivity despite exchange of the gp160 membrane-spanning domain. *Virology 218*, 269−274.
(60) Miyauchi, K., Curran, R., Matthews, E., Komano, J., Hoshino, T., Engelman, D. M., and Matsuda, Z. (2006) Mutations of conserved glycine residues within the membrane-spanning domain of Human Immunodeficiency Virus type 1 gp41 can inhibit membrane fusion and incorporation of Env onto virions. *Jpn. J. Infect. Dis. 59*, 77−84.
(61) Reuven, E. M., Dadon, Y., Viard, M., Manukovsky, N., Blumenthal, R., and Shai, Y. (2012) HIV-1 gp41 transmembrane domain interacts with the fusion peptide: Implication in lipid mixing and inhibition of virus-cell fusion. *Biochemistry 51*, 2867−2878.